PHYSICAL REVIEW B **81**, 014422 (2010)

Anisotropic magnetic field responses of ferroelectric polarization in the trigonal multiferroic $CuFe_{1-x}Al_xO_2$ ($x=0.015$)

Taro Nakajima,* Setsuo Mitsuda, Shunsuke Kanetsuki, Motoyoshi Yamano, and Shunsuke Iwamoto
Department of Physics, Faculty of Science, Tokyo University of Science, Tokyo 162-8601, Japan

Yukihiko Yoshida
Department of Applied Physics, Faculty of Science, Tokyo University of Science, Tokyo 162-8601, Japan

Hiroyuki Mitamura, Yoshiki Sawai, Masashi Tokunaga, and Koichi Kindo
Institute for Solid State Physics, University of Tokyo, Kashiwa 277-8581, Japan

Karel Prokeš and Andrey Podlesnyak
Helmholtz-Centre Berlin for Materials and Energy, SF-2, Glienicker Straße 100, Berlin 14109, Germany
(Received 2 October 2009; published 26 January 2010)

We have investigated magnetic field dependences of a ferroelectric incommensurate-helimagnetic order in a trigonal magnetoelectric multiferroic $CuFe_{1-x}Al_xO_2$ with $x=0.015$, which exhibits the ferroelectric phase as a ground state, by means of neutron diffraction, magnetization, and dielectric polarization measurements under magnetic fields applied along various directions. From the present results, we have established the *H-T* magnetic phase diagrams for the three principal directions of magnetic fields; (i) parallel to the *c* axis, (ii) parallel to the helical axis, and (iii) perpendicular to the *c* and the helical axes. While the previous dielectric polarization (P) measurements on $CuFe_{1-x}Ga_xO_2$ with $x=0.035$ have demonstrated that the magnetic field dependence of the "magnetic domain structure" results in distinct magnetic field responses of P [S. Seki *et al.*, Phys. Rev. Lett. **103**, 237601 (2009)], the present study have revealed that the anisotropic magnetic field dependence of the ferroelectric helimagnetic order "in each magnetic domain" can be also a source of a variety of magnetic field responses of P in $CuFe_{1-x}A_xO_2$ systems ($A=$Al, Ga).

DOI: 10.1103/PhysRevB.81.014422 PACS number(s): 75.80.+q, 75.25.−j, 77.80.−e

I. INTRODUCTION

Nonlinear magnetoelectric (ME) effects, in particular, magnetic field control of ferroelectric polarization (P), in ME multiferroics have been intensively studied since the discovery of the colossal ME effect in some magnetically frustrated transition-metal oxides.[1–5] In most of the ME multiferroics, the magnetic field dependences of P have been attributed to changes in the magnetic structures. For example, the magnetic field-induced 90° flop of P in $TbMnO_3$ has been explained by the first-order magnetic phase transition from the *bc*-plane cycloidal magnetic ordering to the *ac*-plane cycloidal magnetic ordering.[6,7] On the other hand, the recent experimental works have pointed out that magnetic control of "magnetic domain structures" can be an another ingredient for the ME effects, in some relatively high-symmetry (trigonal, tetragonal, or hexagonal) multiferroics.[8–11] For example, Kimura *et al.* have argued that an anisotropic magnetic field dependence of P in a trigonal ME multiferroic $CuCrO_2$ can be ascribed to the magnetic field dependence of the volume fractions of the three magnetic domains in which the three magnetic modulation wave vectors characterizing these domains are equivalent to each other because of the trigonal symmetry of the crystal structure.[8] This suggests that trigonal (or tetragonal, hexagonal) ME multiferroics can provide opportunities for realizing a variety of magnetic field responses of P.

In the past several years, a trigonal ME multiferroic $CuFeO_2$ (CFO) has been the subject of increasing interest as a ME multiferroic because of the discovery of the ferroelectricity in a magnetic field-induced phase.[12] Subsequent studies have elucidated that the ferroelectric phase is stabilized even under zero magnetic field by substituting small amount of nonmagnetic Al^{3+} or Ga^{3+} ions for the magnetic Fe^{3+} ions.[13–15] The magnetic structure in the ferroelectric phase has been determined to be a proper-screw-type helical magnetic structure.[16] The magnetic modulation wave vector is $(q,q,\frac{3}{2})$ where $q=0.202-0.210$, and the helical axis is parallel to the [110] axis.[16,17] Hereafter, we refer to the ferroelectric phase as ferroelectric incommensurate-magnetic (FE-ICM) phase. Recent polarized neutron diffraction studies have revealed that the spin helicity, left-handed or right-handed helical arrangement of spins, determines the polarity of the local ferroelectric polarization emerging along the helical axis.[17,18] Because of the threefold rotational symmetry about the hexagonal *c* axis [see Fig. 1(a)], the magnetic ordering with the wave vector of $(q,q,\frac{3}{2})$ results in three magnetic domains whose wave vectors of $(q,q,\frac{3}{2})$, $(q,-2q,\frac{3}{2})$, and $(-2q,q,\frac{3}{2})$ are crystallographically equivalent to each other, as illustrated in Fig. 1(c). In this paper, we refer to these three domains as "q domains."

Quite recently, Seki *et al.*[11] have reported that the magnetic domain structure in the FE-ICM phase, specifically the volume fractions of the three q domains, can be controlled by applying a magnetic field in the triangular lattice plane. They performed magnetization and dielectric polarization measurements on $CuFe_{1-x}Ga_xO_2$ (CFGO) with $x=0.035$, in which the FE-ICM phase shows up as a ground state, under

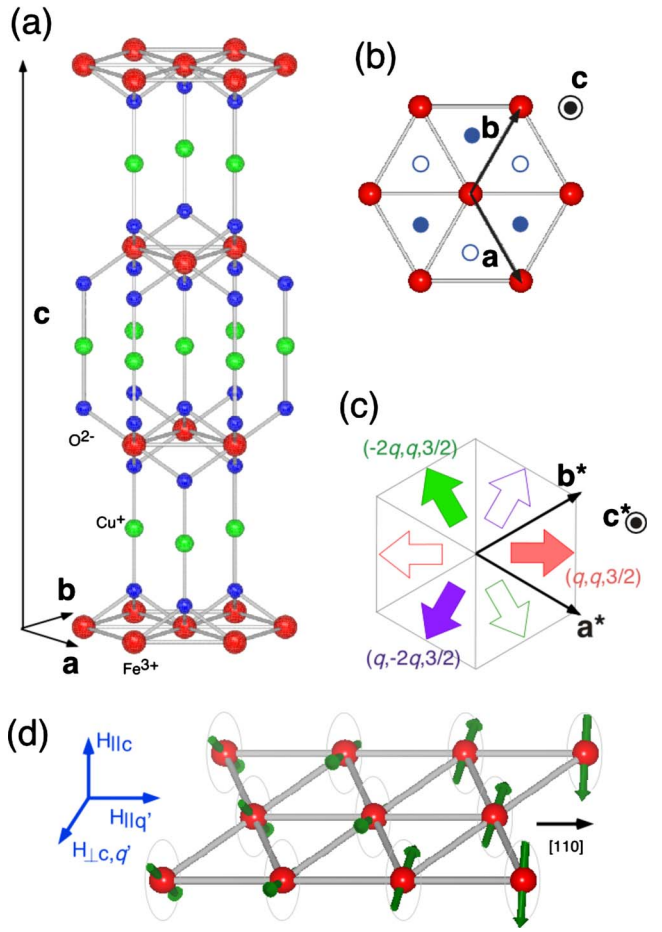

FIG. 1. (Color online) (a) Crystal structure of $CuFeO_2$. (b) The definitions of the hexagonal basis and the arrangements of the O^{2-} ions above (open blue circles) and below (filled blue circles) a Fe^{3+} triangular lattice layer. (c) Schematic drawing of the q' vectors of the three q domains and the reciprocal-lattice basis. (d) Illustration of the magnetic structure in the FE-ICM phase and the directions of $H_{\|c}$, $H_{\|q'}$, and $H_{\perp c,q'}$.

various magnitudes and directions of magnetic fields. These measurements revealed that the "in-plane" magnetic field dependence of the volume fractions of the q domains results in distinct magnetic field responses of P, for example, 120° flop of P by the magnetic fields rotating in the c plane. However, magnetic field dependence of the magnetic ordering "in each q domain" was not discussed because it is quite difficult to extract the information on the magnetic ordering in each q domain from the results of the macroscopic polarization or magnetization measurements. In order to completely understand magnetic field dependences of P in slightly diluted CFO systems, therefore, it is critical to elucidate both of the magnetic field dependences of the "magnetic ordering in each q domain" and the magnetic domain structure.

In the present study, we have investigated magnetic field dependences of P and the FE-ICM order in $CuFe_{1-x}Al_xO_2$ (CFAO) with $x=0.015$, which exhibits the FE-ICM phase as a ground state, by means of neutron diffraction, magnetization, and dielectric polarization measurements under various directions of magnetic fields. In order to elucidate the magnetic field dependence of the FE-ICM order "in a q domain," we have established H-T magnetic phase diagrams for the three principal directions of magnetic fields, specifically, (i) parallel to the c axis, (ii) parallel to the helical axis, and (iii) perpendicular to the c and the helical axes. The present results have revealed that the anisotropic magnetic field dependence of the FE-ICM order in each q domain results in a variety of magnetic field responses of P as well as the magnetic field dependence of the magnetic domain structure does.

We have also investigated a magnetic field dependence of sensitivity of P to a poling electric field (E_p). In our previous polarized neutron diffraction and *in situ* pyroelectric measurements on CFAO($x=0.015$) and CFGO($x=0.035$) in zero field, we have found that the Al substitution more significantly reduced the sensitivity of P to E_p as compared to the Ga substitution.[17] These measurements have also revealed that CFGO($x=0.035$) exhibits a homogeneous FE-ICM state, that is relatively close to the long-range-ordered state, in contrast to CFAO($x=0.015$), that has an inhomogeneous domain state in zero field.[17] We have thus concluded that the "inhomogeneity" of the FE-ICM order, which must be relevant to the mobility of the magnetic domain walls, determines the sensitivity of P to E_p. On the other hand, our previous neutron-diffraction measurements under applied magnetic fields showed that the homogeneous FE-ICM state can be realized even in CFAO($x=0.015$) by applying a magnetic field along the c axis.[16] Therefore, the sensitivity of P to E_p in CFAO($x=0.015$) is expected to be controlled by an application of a magnetic field. This is the reason why we have selected CFAO($x=0.015$) sample for the present study.

This paper is organized as follows. In Sec. II, we describe experimental details. Section III consists of two subsections. In Sec. III A, we present anisotropic H-T magnetic phase diagrams for a q domain using the results of the neutron-diffraction measurements under the three directions of the magnetic fields, and also present the results of pyroelectric measurements under steady magnetic fields. In Sec. III B, we present magnetic field variations in P and the FE-ICM order using the results of neutron diffraction, magnetization, and dielectric polarization measurements under magnetic fields. In Sec. IV, we summarize our conclusions.

II. EXPERIMENTAL DETAILS

Single crystal of $CuFe_{1-x}Al_xO_2$ with $x=0.015$ was prepared by the floating-zone technique.[19] For the measurements of P, the sample was cut into a thin plate ($\sim 2\times 4\times 0.1$ mm^3). Silver paste was applied on the $[1\bar{1}0]$ surface of the sample to form the electrodes. In the pyroelectric measurements under steady magnetic fields, the pyroelectric current was measured under zero electric field with increasing temperature, using an electrometer (Keithley 6517A). Before each pyroelectric measurement, we performed cooling with an applied poling electric field (E_p) from 15 to 2 K. After the poling electric field was removed at 2 K, the sample was allowed to discharge for about 40 min in order to reduce residual current. The typical magnitude of E_p in the present pyroelectric measurements was ~ 250 kV/m. We also investigated the E_p dependence of P up to $E_p=2.0$ MV/m. Exter-

nal magnetic fields up to 5 T were provided by the magnetic property measurement system (Quantum Design Inc.).

We have performed dielectric polarization and magnetization measurements on CFAO(x=0.015) under pulsed magnetic fields. The pulsed high magnetic fields up to 55 T were generated by a nondestructive magnet in the International MegaGauss Science Laboratory in ISSP, the University of Tokyo. The magnetization along the field direction was measured by the induction method using coaxial pick-up coils. The dimensions of the single-crystal sample used for the magnetization measurements were $1.8\times1.8\times2.3$ mm^3. Following the pioneer work on the dielectric polarization measurement under pulsed magnetic fields by Mitamura *et al.*,[20] we detected the H-induced change in P by monitoring the polarization current through a voltage drop in the shunt resistance connected in series. By integrating the current with respect to time, we obtained the magnetic field variations in P. In this measurement, the poling electric fields (E_p) were continuously applied during all the measurements of the P-H curve. The magnitude of E_p was typically $\sim$200 kV/m. The single-crystal sample for this measurement was identical to the sample used for the present pyroelectric measurements.

The neutron-diffraction measurements under applied field were carried out at the two-axis neutron diffractometer E4 installed at Berlin Neutron Scattering Center (BENSC) in Helmholtz Centre Berlin for Materials and Energy. A typical dimension of the single-crystal samples for the neutron experiments was $\sim3\times4\times4.5$ mm^3. External magnetic fields along the hexagonal [001], [110], and [1$\bar{1}$0] directions were provided by the cryomagnets HM-1, HM-2, and VM-1, whose maximum fields are 6, 4, and 14.5T, respectively. Note that the magnetic field along [001] axis was canted by $\sim$12° from the [001] axis toward [110] axis, because of limitations of the windows of the horizontal field cryomagnet HM-1. For all the neutron-diffraction measurements, the sample was mounted in the cryomagnet with a (h,h,l) scattering plane. In the experiments with the [001] and [1$\bar{1}$0] magnetic fields, the collimation was 40′-40′-40′, and a single detector was used. In the experiment with the [110] magnetic field, the collimation was 40′-40′ open, and a two-dimensional position-sensitive detector was used. In this paper, we have employed a conventional hexagonal basis defined as shown in Fig. 1(a), in order to describe the directions of the magnetic propagation vectors of the three q domains, although structural transitions from the original trigonal structure to a monoclinic structure have been reported for some of the magnetically ordered phases (including the FE-ICM phase) of $CuFeO_2$ (Refs. 21–23) and $CuFe_{1-x}Al_xO_2$.[24]

III. RESULTS AND DISCUSSIONS

A. Magnetic field dependence of the phase transitions in a q domain

1. Neutron-diffraction measurements under steady magnetic fields

We first investigated the temperature variations in the magnetic ordering in a q domain under steady magnetic fields by means of the neutron-diffraction measurements. In order to define the relationship between the directions of the magnetic fields and the magnetic structure in a q domain, we introduce the c-plane projection of the q vector, $q'=(q,q,0)$. In the present neutron-diffraction measurements, we applied magnetic fields along the three directions; (i) nearly parallel to the [001] axis,[25] (ii) parallel to the [110] axis, and (iii) parallel to the [1$\bar{1}$0] axis. Since the magnetic reflections on the (h,h,l) scattering plane belong to the q domains with the wave vector of $(q,q,\frac{3}{2})$, the directions of the [110] axis corresponds to the q' vector of the $(q,q,\frac{3}{2})$ domain. Hereafter, we refer to the magnetic fields along these three directions as $H_{\|c}$, $H_{\|q'}$, and $H_{\perp c,q'}$ [see Fig. 1(d)].

Before discussing the present results, we should review the magnetic phase transitions in CFAO(x=0.015) in zero magnetic field. As reported by Terada *et al.*,[26] CFAO(x=0.015) has three magnetically ordered phases in zero magnetic field. The typical magnetic diffraction profiles of the $(h,h,\frac{3}{2})$ reciprocal lattice scans in zero field are shown in Fig. 2 by black filled circles. With decreasing temperature from the paramagnetic phase, two collinear-incommensurate magnetic phases show up; the higher temperature phase is the oblique partially disordered (OPD) phase and the lower temperature phase is the PD phase. Both of the magnetic reflections corresponding to the OPD and PD magnetic orderings are assigned as $(q,q,\frac{3}{2})$. The incommensurate wave number for the OPD phase, $q_{\mathrm{OPD}}\sim0.195$ is almost independent of temperature, while that for the PD phase, q_{PD}, varies from 0.20 to 0.22 with decreasing temperature. Previous neutron-diffraction measurements by Terada *et al.*[26,27] have revealed that the magnetic moments in the PD and OPD phases are canted by about 12°, 50° from the [001] direction toward the [1$\bar{1}$0] direction, respectively. The ground state of CFAO(x=0.015) is the FE-ICM phase, as mentioned in Sec. I. The magnetic diffraction profile in the FE-ICM phase is characterized by the two magnetic reflections assigned as $(q,q,\frac{3}{2})$ and $(\frac{1}{2}-q,\frac{1}{2}-q,\frac{3}{2})$ (Ref. 28) using the hexagonal basis, as shown in Fig. 2(a-4). The magnetic modulation wave number in the FE-ICM phase, $q_{\mathrm{FE\text{-}ICM}}=0.202-0.210$, slightly depends on the Al concentration and applied magnetic fields, but is almost independent of temperature. It should be noted that a small peak at $(\frac{1}{4},\frac{1}{4},\frac{3}{2})$ corresponds to the collinear-commensurate four-sublattice phase, which coexists with the FE-ICM phase at low temperatures because of a slight macroscopic inhomogeneity of the Al concentration in the samples.[26]

We now discuss the results of the present neutron-diffraction measurements under applied magnetic fields. In Fig. 2, we show the magnetic diffraction profiles measured on cooling under $H_{\|c}$, $H_{\|q'}$, and $H_{\perp c,q'}$ of 4 T. In all the three cooling, the successive magnetic transitions [OPD$\rightarrow$PD$\rightarrow$FE-ICM] were observed, and no strong magnetic field dependences of the magnetic diffraction profiles were found in the OPD and PD phase, although the wave number of the PD phase is slightly dependent on $H_{\|c}$. However, we found that the magnetic diffraction profiles in the FE-ICM phase under $H_{\|c}$, $H_{\|q'}$, and $H_{\perp c,q'}$ are remarkably different from each other, as shown in Fig. 2(a-4), 2(b-4) and 2(c-4).

Figure 2(b-4) shows the magnetic diffraction profile in the FE-ICM phase under $H_{\|q'}$, suggesting that the magnetic field

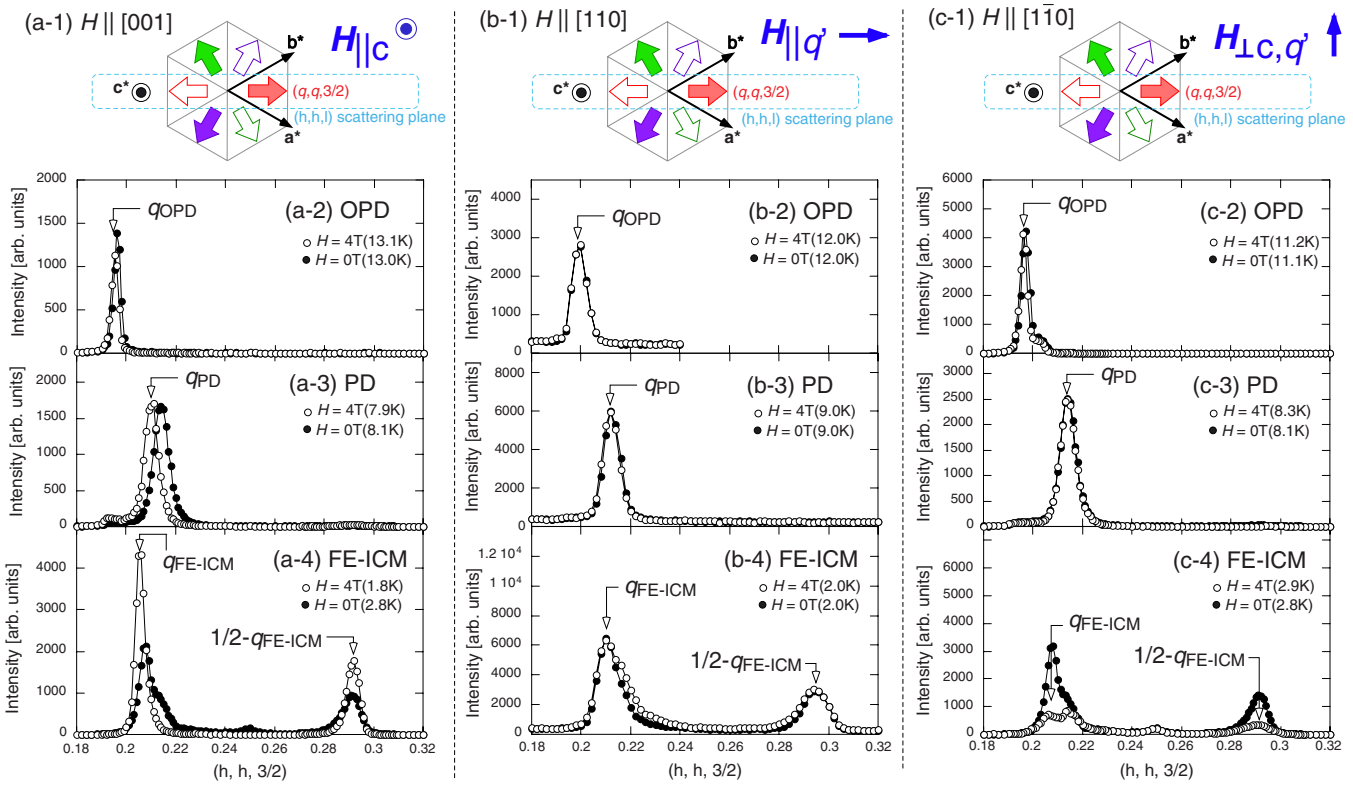

FIG. 2. (Color online) [(a-1), (b-1), and (c-1)] The relationships between the applied magnetic fields and q' vector of the q domain observed in the present neutron-diffraction measurements under (a-1) $H_{\parallel c}$, (b-1) $H_{\parallel q'}$, and (c-1) $H_{\perp c,q'}$. The magnetic diffraction profiles measured in the cooling processes under [(a-2)–(a-4)] $H_{\parallel c}$, [(b-2)–(b-4)] $H_{\parallel q'}$, and [(c-2)–(c-4)] $H_{\perp c,q'}$. The data observed in the magnetic fields are shown by the open circles, and those in zero field are shown by the black filled circles. Note that the difference in the width of the magnetic diffraction profiles between the measurements under $H_{\parallel q'}$ and the others is due to the different experimental configurations, specifically the collimations and the detectors. See Sec. II for details.

applied along the helical axis does not result in the drastic change in the FE-ICM order. In contrast, the magnetic fields applied perpendicular to the helical axis, $H_{\parallel c}$ and $H_{\perp c,q'}$, significantly affect the magnetic diffraction profiles in the FE-ICM phase. Figure 2(a-4) shows that $H_{\parallel c}$ sharpens the magnetic diffraction profile in the FE-ICM phase, as was partly reported in Ref. 16. This suggests that the FE-ICM order under $H_{\parallel c}$ is relatively close to the long-range-ordered state,

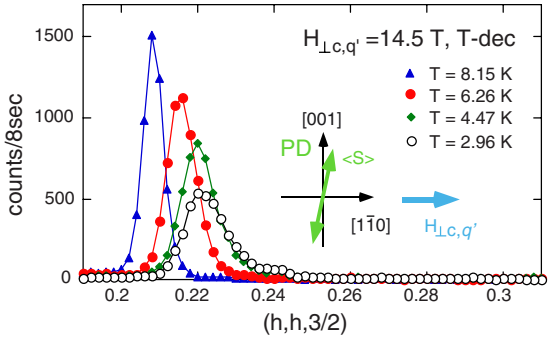

FIG. 3. (Color online) The temperature variation in the magnetic diffraction profile of the $(h,h,\frac{3}{2})$ reciprocal lattice scans under $H_{\perp c,q'}$ of 14.5 T. Inset shows relationship between the directions of $H_{\perp c,q'}$ and the magnetic moments of the PD magnetic order in zero field.

while the FE-ICM order is inhomogeneous domain state in zero magnetic field,[17] as mentioned in Sec. I. This $H_{\parallel c}$ dependence of the magnetic correlation might be attributed to the local lattice distortions due to the Al substitution.

The previous studies on CFAO (Ref. 17) and CFGO (Refs. 15 and 17) have pointed out that the Al substitution should result in local lattice distortions because the ionic radius of Al^{3+} is much smaller than that of Fe^{3+}, and have also suggested that this local lattice distortion strongly disturbs a coherent magnetic ordering in the FE-ICM phase because the distortions randomly lift the local degeneracy in the competing exchange interactions. On the other hand, the previous synchrotron radiation x-ray diffraction measurements on pure CFO under applied magnetic fields revealed that the lattice constants in the FE-ICM phase vary with $H_{\parallel c}$;[23,29] specifically, the lattice constant along the [110] direction, which is the b axis in the monoclinic notation, linearly decreases with increasing $H_{\parallel c}$. Taking account of these results, one can expect that the local lattice distortion relaxes with increasing $H_{\parallel c}$. For further investigation on this problem, x-ray diffraction measurements on CFAO system under applied magnetic fields are required.

In contrast to $H_{\parallel c}$, in the cooling process under $H_{\perp c,q'}$, the magnetic diffraction corresponding to the FE-ICM order is rather diffusive. This implies that the FE-ICM order is suppressed by $H_{\perp c,q'}$. Actually, as shown in Fig. 3, the PD to

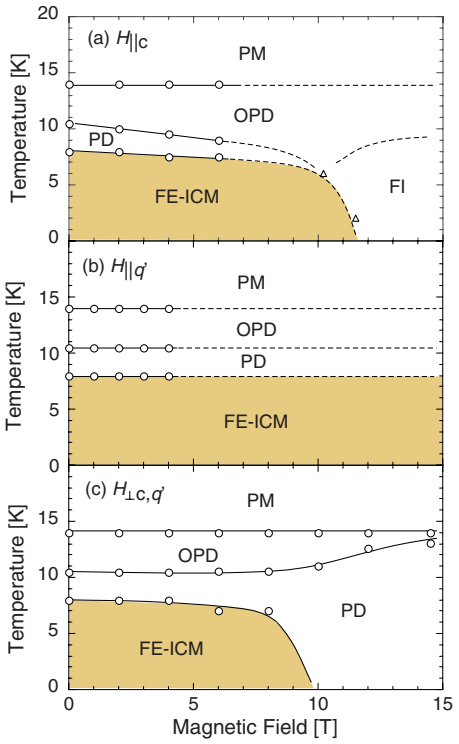

FIG. 4. (Color online) [(a)–(c)] The H-T magnetic phase diagrams for (a) $H_{\|c}$, (b) $H_{\|q'}$, and (c) $H_{\perp c,q'}$. Open circles and solid lines denote the phase boundaries determined by the present neutron-diffraction measurements on cooling. The phase boundaries in the high-field region of the $H_{\|c}$-T phase diagram (dashed lines) were drawn in analogy of the $H_{\|c}$-T phase diagram of CFAO(x =0.02) (Ref. 30). To check the reasonability of the phase boundaries in (a), we have shown the transition field between the FE-ICM phase and the FI phase determined by the dielectric polarization measurements under pulsed magnetic fields presented in Sec. III B 2 (open triangles).

FE-ICM magnetic phase transition is not detected in the cooling process under $H_{\perp q',c}$=14.5 T, and instead, the PD magnetic ordering survives even at 2.9 K. This suggests that $H_{\perp c,q'}$ favors the PD magnetic ordering, whose magnetic moments lie nearly perpendicular to the magnetic field, rather than the proper-screw-type magnetic order in the FE-ICM phase.

2. H-T magnetic phase diagram for $H_{\|c}$, $H_{\|q'}$, and $H_{\perp c,q'}$

In Figs. 4(a)–4(c), we now present the H-T magnetic phase diagrams for $H_{\|c}$, $H_{\|q'}$, and $H_{\perp c,q'}$ deduced from the present results. Although the present neutron-diffraction measurements could not reach the high-field region of the $H_{\|q'}$-T phase diagram, we have confirmed that the FE-ICM phase extends to the high-field region by the present dielectric polarization measurements under pulsed magnetic fields up to 30 T to be mentioned in Sec. III B 2. Here, we should emphasize that these phase diagrams represent the magnetic ordering in a q domain, and moreover, those revealed that the FE-ICM order in a q domain shows the anisotropic responses for the in-plane magnetic fields of $H_{\|q'}$ and $H_{\perp c,q'}$, which was not directly observed in the previous macroscopic polarization and magnetization measurements.[11]

3. Pyroelectric measurements in steady magnetic fields

We have also performed pyroelectric measurements under applied magnetic fields to observe the magnetic field dependences of P corresponding to the FE-ICM order observed in the present neutron-diffraction measurements. As mentioned in Sec. I, the direction of the spontaneous electric polarization in the FE-ICM order is parallel to the helical axis,[18] that is, the direction of the q' vector. In addition, the previous polarized neutron-diffraction measurement under applied electric field revealed that an application of a poling electric field cannot result in a single q-domain state.[17,18] Therefore, the measured electric polarization has to be the sum of the contributions from the domains with the different q vectors. This situation prevent us from investigating the anisotropic ME responses in a q domain by pyroelectric measurements.

To overcome this problem, we have thus selected the [120] plane, which is crystallographically equivalent to the $[1\bar{1}0]$ and $[\bar{2}\bar{1}0]$ planes, as the electrode surfaces, and applied magnetic fields along three principal directions; (i) parallel to the c axis, (ii) parallel to the poling electric field (E_p), and (iii) perpendicular to the c axis and E_p. We refer to these three directions of the magnetic fields as $H_{\|c}$, $H_{\|E_p}$, and $H_{\perp c,E_p}$, respectively. The directions of the poling electric field, the q' vectors of the three domains and the applied magnetic fields are schematically drawn in Figs. 5(a-1), 5(b-1), and 5(c-1). In this configuration of the electrodes, only the two q domains with the wave vectors of $(q,q,\frac{3}{2})$ and $(q,-2q,\frac{3}{2})$ contribute to the measured electric polarization, because the electric polarization vector in the $(-2q,q,\frac{3}{2})$ domain is perpendicular to the normal vector of the electrode surfaces. In addition, the $H_{\|E_p}$ (or $H_{\perp c,E_p}$) dependence of the FE-ICM order in the $(q,q,\frac{3}{2})$ domains is expected to be the same as that in the $(q,-2q,\frac{3}{2})$ domains because of the symmetry of the crystal and magnetic structures. By this configuration of the electrodes, the anisotropic in-plane field dependences of P can be observed.

Figures 5(b-2), and 5(c-2) show the temperature variations in P under $H_{\|E_p}$ and $H_{\perp c,E_p}$. For both of $H_{\|E_p}$ and $H_{\perp c,E_p}$, the magnitude of P decreased with increasing magnetic field. Taking account the present neutron-diffraction measurements revealing that the FE-ICM order was significantly affected by $H_{\perp c,q'}$ and was less affected by $H_{\|q'}$, we conclude that the $H_{\perp c,q'}$ components of the magnetic fields are relevant to the reduction in P. Actually, $H_{\perp c,E_p}$ more remarkably reduced P than $H_{\|E_p}$. We thus show, in Fig. 5(e), the values of P at T=2 K normalized to the values in zero magnetic field as a function of the effective magnetic field applied perpendicular to the c axis and the q' vector, $H^{eff}_{\perp c,q'}$ [see Fig. 5(d)], specifically

$$H^{eff}_{\perp c,q'} = H_{\perp c,E_p} \cos 30^\circ = H_{\|E_p} \sin 30^\circ . \quad (1)$$

We found that the $H_{\perp c,E_p}$ and $H_{\|E_p}$ dependences of P at T =2.0 K are scaled by $H^{eff}_{\perp c,q'}$. This clearly shows that $H_{\perp c,q'}$ dominates the in-plane magnetic field dependence of P, as was expected from the results of the present neutron-diffraction measurements.

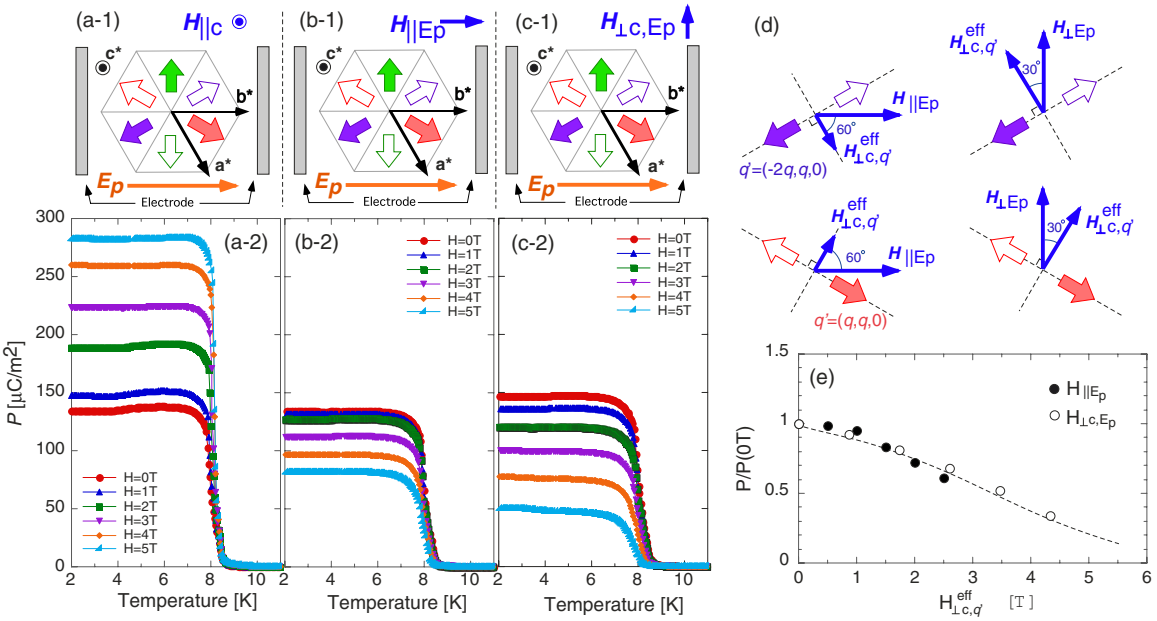

FIG. 5. (Color online) [(a-1), (b-1), and (c-1)] The relationships between the applied magnetic fields and q' vectors for (a-1) $H_{\|c}$, (b-1) $H_{\|E_p}$, and (c-1) $H_{\perp c,E_p}$. The magnetic field dependence of the temperature variations in P under (a-2) $H_{\|c}$, (b-2) $H_{\|E_p}$, and (c-2) $H_{\perp c,E_p}$. (d) The definition of the $H^{eff}_{\perp c,E_p}$ for the in-plane magnetic fields of $H_{\|E_p}$ and $H_{\perp c,E_p}$. (e) The $H^{eff}_{\perp c,E_p}$ dependences of P at 2.0 K normalized to the value of P in zero field. The dashed line is the guide to eyes.

As for the origin of the reduction in P under a magnetic field having the $H_{\perp c,q'}$ component, we can propose three possibilities; the first one is that the volume fraction of the FE-ICM order in each q domains was reduced because of the PD magnetic order retained by the magnetic field, the second is that the magnetic structure of the FE-ICM order was partly modified by the magnetic field, and the third is that the sensitivity of P to E_p was reduced because of the reduction in the coherence of the magnetic order in the FE-ICM phase under the magnetic field. A combination of two or three of them is also possible. Although we cannot identify the origin of the reduction in P only from the present results but the E_p dependence of P in $H_{\perp c,E_p}$=5 T shown in Fig. 6 suggests that the third scenario contributes to the reduction in P.

In Fig. 5(a-2), we show the temperature variations in P under $H_{\|c}$. In contrast to the in-plane magnetic fields, the application of $H_{\|c}$ enhances P. Moreover, Fig. 6 shows that the sensitivity of P to E_p was significantly enhanced by applying $H_{\|c}$. As mentioned in Sec. I, the previous study on CFAO and CFGO has revealed that the sensitivity of P to E_p is determined by the inhomogeneity of the FE-ICM order, that must be relevant to the mobility of the magnetic domain walls in the FE-ICM phase.[17] Taking account of the present neutron-diffraction measurements revealing that CFAO(x=0.015) exhibits the long-range-ordered FE-ICM phase above $H_{\|c}$=4 T, we attributed to the enhanced sensitivity of P to E_p to the $H_{\|c}$ dependence of the magnetic correlation in the FE-ICM phase.

Note that the curvatures of the E_p dependence of P implies that the saturation value of P was also enhanced by $H_{\|c}$. This might be ascribed to the $H_{\|c}$ dependence of the (local) magnetic structure including the wave number of the magnetic order in the FE-ICM phase.

B. Magnetic field variations in the FE-ICM order

1. Neutron-diffraction measurements under applied magnetic field

On the basis of the results of the field-cooling scans, we now discuss magnetic field variations in the FE-ICM order including those of the domain structure. According to the $H_{\perp c,q'}$-T phase diagram shown in Fig. 4(c), the magnetic phase transition from the noncollinear FE-ICM phase to the collinear PD phase is expected in a $H_{\perp c,q'}$-increasing process. Figures 7(a-1) and 7(b-1) show the $H_{\perp c,q'}$ variations in the neutron-diffraction profiles measured at T=6.0 and 2.8 K, respectively. In the magnetic field scan at T=6.0 K, the

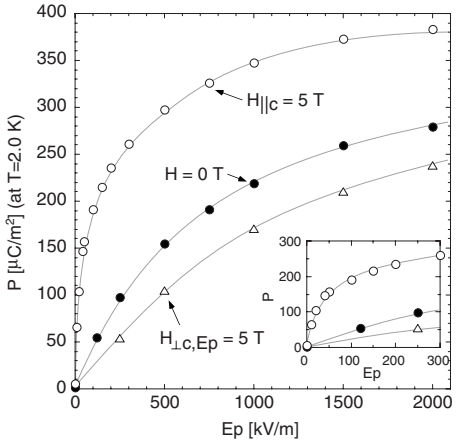

FIG. 6. The E_p dependences of the values of P at T=2.0 K in zero field under $H_{\|c}$=5.0 T and $H_{\perp c,E_p}$=5.0 T. The inset shows the magnification of the region of $0<E_p<300$ kV/m. The solid gray lines are guides to eyes.

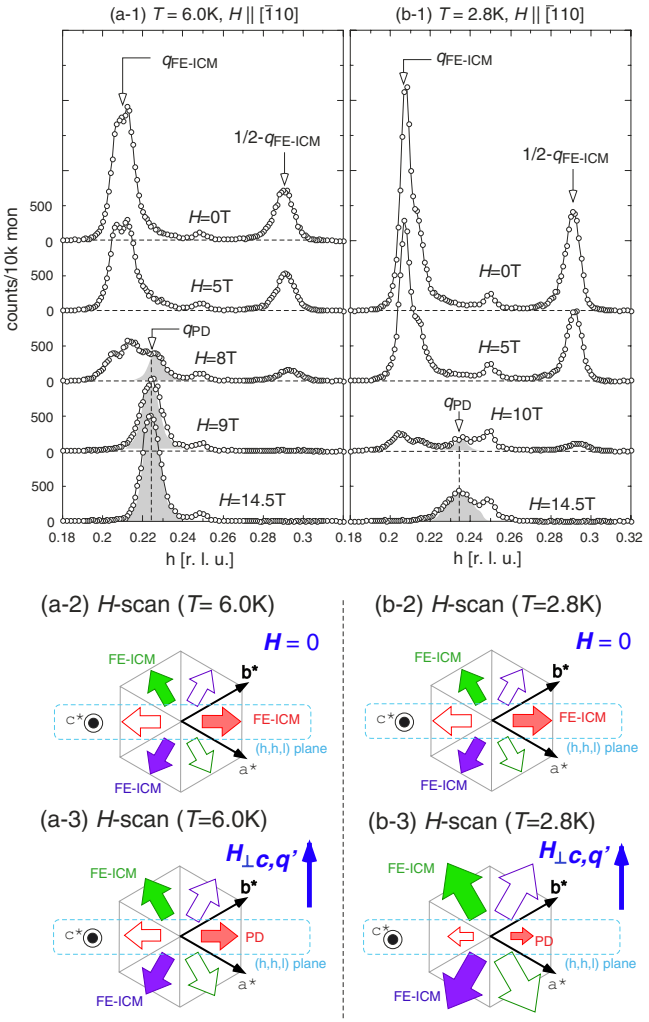

FIG. 7. (Color online) [(a-1) and (b-1)] The $H_{\perp c,q'}$ variations in the neutron-diffraction profiles of the $(h,h,\frac{3}{2})$ reciprocal lattice scans at (a-1) 6.0 and (b-1) 2.8 K. [(a-2), (a-3), (b-2), and (b-3)] Schematic drawings of the $H_{\perp c,q'}$-induced magnetic phase transitions in each q domain. The sizes of the arrows qualitatively show the volume fractions of the q domains.

intensities of the magnetic reflections corresponding to the FE-ICM order monotonically decrease with increasing $H_{\perp c,q'}$, and disappear around 9.0 T, as expected from the phase diagram. On the other hand, magnetic reflections described by the wave vector of the PD phase, $(q_{\mathrm{PD}},q_{\mathrm{PD}},\frac{3}{2})$ with $q_{\mathrm{PD}}\sim 0.22$, emerge above 8.0 T. This result apparently manifests the magnetic field-induced phase transition from the FE-ICM phase to the PD phase.

In the magnetic field scan at $T=2.8$ K, the field-induced magnetic transition was also observed, as shown in Fig. 7(b-1). However, we found that the diffraction profile of the field-induced PD phase is rather diffusive. This indicates that the sinusoidally amplitude-modulated magnetic structure of the PD phase is no longer stable at low temperatures. In addition, we also found that the intensity corresponding to the field-induced PD magnetic order is considerably small. This implies that the volume fraction of the $(q,q,\frac{3}{2})$ domains is reduced by the applied magnetic field, namely, that the

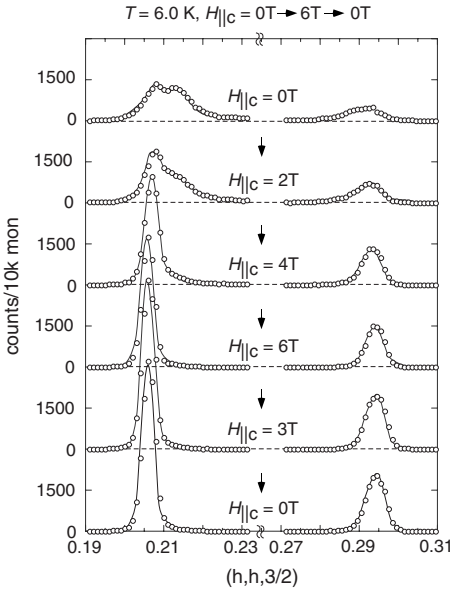

FIG. 8. The $H_{\|c}$ variation in the neutron-diffraction profiles of the $(h,h,\frac{3}{2})$ reciprocal lattice scans at $T=6.0$ K.

volume fractions of the three q domains are changed by $H_{\perp c,q'}$, as illustrated in Figs. 7(b-2) and 7(b-3). This indicates that at low temperature, the in-plane magnetic field favors the proper helical magnetic domains whose helical axis follows it, as demonstrated in the previous works.[11,24]

To summarize the $H_{\perp c,q'}$ dependence of the magnetic ordering in this system, the magnetic phase transition from the FE-ICM phase to the PD phase is observed at the relatively high temperature ($T=6.0$ K), and the repopulation of the q domains occurs at low temperatures ($T=2.8$ K). As mentioned in Sec. I, Seki *et al.* have demonstrated that a magnetic field rotating in the triangular lattice plane can induce 120° flop of the electric polarization because of the repopulation of the q domains.[11] The maximum magnitude of the rotating magnetic field shown in Ref. 11 was 6.5 T and the measurements were carried out at 2.0 K. However, the present results suggest that more diversity in the ME responses should be found by applying magnetic fields beyond ~9 T and by changing the temperature.

Figure 8 shows the $H_{\|c}$ variation in the neutron-diffraction profiles at $T=6.0$ K. As seen in the field-cooling scans, the magnetic field applied along the c axis sharpens the magnetic diffraction profile. In addition, the wave number of the FE-ICM order, which was distributed around $q\sim 0.21$ in zero field, was concentrated at $q=0.207$ above $H_{\|c}=4$ T. We also found that the sharp magnetic diffraction profiles retained after removing the magnetic field. This history-dependent behavior indicates the long-range magnetic ordering realized by the application of $H_{\|c}$ remained even after returning to the zero field.

2. Magnetization and dielectric polarization measurements under pulsed magnetic fields

We also performed the dielectric polarization and magnetization measurements under pulsed magnetic field up to 30 T. The electrode configuration and the magnetic field direc-

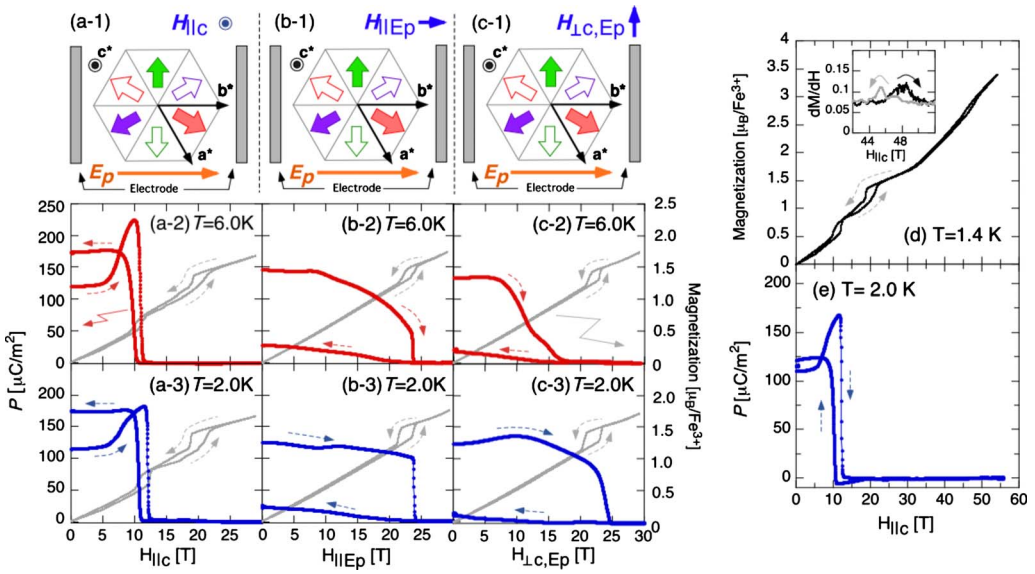

FIG. 9. (Color online) [(a-1), (b-1), and (c-1)] The relationships between the directions of E_p, the q' vectors and the applied magnetic fields of (a-1) $H_{\|c}$, (b-1) $H_{\|E_p}$, and (c-1) $H_{\perp c,E_p}$. The results of the polarization and magnetization measurements under the pulsed magnetic fields of [(a-2) and (a-3)] $H_{\|c}$, [(b-2) and (b-3)] $H_{\|E_p}$, and [(c-2) and (c-3)] $H_{\perp c,E_p}$. [(d) and (e)] The $H_{\|c}$ dependence of the magnetization and P in CFAO(x=0.015) up to 55 T. The inset shows the $H_{\|c}$ dependence of $dM/dH_{\|c}$ around the fifth field-induced phase transition.

tions were selected to be the same as those in the pyroelectric measurements discussed in Sec. III A 3.

We first discuss the metamagnetic transition in this system using the results of the magnetization measurements. In $H_{\|c}$ up to 30 T, three magnetic phases appear, as shown in Figs. 9(a-2) and 9(a-3). In the previous work on CFAO(x=0.02),[30] Terada *et al.* have reported that the first field-induced phase from the FE-ICM phase is the slightly incommensurate magnetic phase referred to as the "FI phase." We thus considered that the first field-induced phase from the FE-ICM phase in CFAO(x=0.015) is the FI phase. Around $H_{\|c}$=20 T, where the induced magnetization approaches $\sim 5/3\mu_B$, the system undergoes further magnetic phase transition. In the in-plane magnetic fields, magnetization plateaus with the magnetization of $\sim 5/3\mu_B$ were also observed around 23 T. Comparing the results of the previous magnetization measurements on pure CFO under pulsed magnetic field,[29] we realize that this magnetic phase is the three-sublattice (3SL) phase, which is also observed in pure CFO.[29]

Let us move on to the results of the dielectric polarization measurements. In $H_{\|c}$, the finite electric polarization was observed only in the FE-ICM phase, as shown in Figs. 9(a-2) and 9(a-3). In the $H_{\|c}$-increasing process, P rapidly increases in the magnetic field region of $5 < H_{\|c} < 12$ T. This enhancement corresponds to the magnetic field dependences of the magnetic correlation and the magnetic modulation wave number, which were observed in the present neutron-diffraction measurements. In the $H_{\|c}$-decreasing process, P is also observed to emerge in the FE-ICM phase. In contrast to the $H_{\|c}$-increasing process, the value of P is almost independent of the magnetic field, and is larger than the value in the zero-field state before the measurement. Judging from the symmetry of the magnetic and crystal structure in this system, it is reasonable to assume that the volume fractions of the three q domains are not changed by $H_{\|c}$. Hence, we ascribed this $H_{\|c}$ variations in P to the history-dependent behavior of the FE-ICM order in a q domain observed in the present neutron-diffraction measurements.

Figures 9(b-3) and 9(c-3) show the in-plane magnetic field dependences of P measured at relatively low temperature, T=2.0 K. From the results of the present neutron-diffraction measurements, it is expected that the magnetic field-induced repopulations of the q domains result in anisotropic magnetic field variations in P. However, the expected anisotropic behaviors are not observed, although the details of the P-$H_{\perp c,E_p}$ and P-$H_{\|E_p}$ curves are slightly different from each other. This result suggests that the sweeping rate of the pulsed magnetic fields were too fast to induce the repopulation of the q domains.

On the other hand, at T=6.0 K, we found that the in-plane field variations in P were quite anisotropic, as shown in Figs. 9(b-2) and 9(c-2). In the $H_{\perp c,E_p}$-increasing process, the value of P started to decrease around 8 T, and disappeared around 15 T, which is far below the transition field to the 3SL phase. In contrast, in the $H_{\|E_p}$-increasing process, the finite value of P is observed up to the transition field to the 3SL phase. These results revealed that the in-plane field-induced FE-ICM to PD transition in a q domain occurs even in the pulsed magnetic fields. It should be noted that this field-induced FE-ICM to PD phase transition is not clearly observed in the magnetization measurement. This is because the FE-ICM to PD phase transition occurs only in the q domains with the wave vectors of $(q,q,\frac{3}{2})$ and $(-q,2q,\frac{3}{2})$ while all the three q domains contributes to the measured magnetization.

We also found that in the $H_{\perp c,E_p}$- and $H_{\|E_p}$-decreasing process, the values of P are significantly smaller compared to the values in zero field before the measurements, in contrast to the $H_{\|c}$-decreasing process, in which P was comparable to the value at the initial state. At this stage, we have no clear

explanation for this result. In order to investigate this point, further neutron-diffraction measurements under applied magnetic fields are required.

In Figs. 9(d) and 9(e), we show the $H_{\|c}$ dependence of the magnetization and P up to 55 T, respectively. Although, in this paper, we do not focus on the high magnetic field behavior in this system, it is worth mentioning here that the fifth magnetic field-induced phase transition, which has been recently found in pure CFO,[31,32] was also observed in CFAO(x=0.015) around H=48 T. No finite electric polarization was detected in the magnetic field-induced phases including the "fifth" phase.

IV. CONCLUSION

We have investigated the magnetic field dependence of the FE-ICM order in the trigonal ME-multiferroic $CuFe_{1-x}Al_xO_2$ with x=0.015 by means of the neutron diffraction, dielectric polarization, and magnetization measurements under the magnetic fields applied along various directions.

We have established the H-T magnetic phase diagrams for the three principal directions of the magnetic fields, $H_{\|c}$, $H_{\|q'}$, and $H_{\perp c,q'}$. It should be emphasized that these H-T phase diagrams represent the magnetic ordering in a q domain, and reveal the anisotropic in-plane magnetic field responses of the FE-ICM order in a q domain, which was not directly observed in the previous macroscopic (bulk) polarization and magnetization measurements.[11]

We have also found that the sensitivity of P to E_p in this system was controlled by applying a magnetic field. This indicates that the inhomogeneity of the FE-ICM order, which is also controlled by an applied magnetic field, is relevant to the sensitivity of P to E_p. This result is consistent with our previous polarized neutron-diffraction study on CFAO(x=0.015) and CFGO(x=0.035).[17]

While the recent dielectric polarization measurements on $CuFe_{1-x}Ga_xO_2$ with x=0.035 by Seki *et al.*[11] have demonstrated that the magnetic field dependence of the "magnetic domain structure," specifically the volume fractions of the three q domains, results in the distinct magnetic field responses of P, the present results have revealed the anisotropic magnetic field dependence of the FE-ICM order in each q domain can be also a source of a variety of the magnetic field dependence of P in this system.

ACKNOWLEDGMENTS

The neutron-diffraction measurement at BENSC was carried out along the Proposals No. PHY-01-2285-DT and No. PHY-01-1878. This work was supported by a Grant-in-Aid for Scientific Research (C), Grant No. 19540377, and a Grant-in-Aid, Grant No. 21.2745, from JSPS, Japan. This work was also supported in part by a Grant-in-Aid for Scientific Research on priority Areas "High Field Spin Science in 100T" (Grant No. 451) from the Ministry of Education, Culture, Sports, Science and Technology (MEXT). The images of the crystal and magnetic structures in this paper were depicted using the software VESTA (Ref. 33) developed by K. Monma.

*nakajima@nsmsmac4.ph.kagu.tus.ac.jp

[1] T. Kimura, T. Goto, H. Shintani, K. Ishizaka, T. Arima, and Y. Tokura, Nature (London) **426**, 55 (2003).
[2] N. Hur, S. Park, P. A. Sharma, J. S. Ahn, S. Guha, and S.-W. Cheong, Nature (London) **429**, 392 (2004).
[3] G. Lawes, A. B. Harris, T. Kimura, N. Rogado, R. J. Cava, A. Aharony, O. Entin-Wohlman, T. Yildrim, M. Kenzelmann, C. Broholm, and A. P. Ramirez, Phys. Rev. Lett. **95**, 087205 (2005).
[4] K. Taniguchi, N. Abe, T. Takenobu, Y. Iwasa, and T. Arima, Phys. Rev. Lett. **97**, 097203 (2006).
[5] Y. Yamasaki, S. Miyasaka, Y. Kaneko, J.-P. He, T. Arima, and Y. Tokura, Phys. Rev. Lett. **96**, 207204 (2006).
[6] N. Aliouane, K. Schmalzl, D. Senff, A. Maljuk, K. Prokes, M. Braden, and D. N. Argyriou, Phys. Rev. Lett. **102**, 207205 (2009).
[7] Y. Yamasaki, H. Sagayama, N. Abe, T. Arima, K. Sasai, M. Matsuura, K. Hirota, D. Okuyama, Y. Noda, and Y. Tokura, Phys. Rev. Lett. **101**, 097204 (2008).
[8] K. Kimura, H. Nakamura, K. Ohgushi, and T. Kimura, Phys. Rev. B **78** 140401(R) (2008).
[9] S. Seki, Y. Onose, and Y. Tokura, Phys. Rev. Lett. **101**, 067204 (2008).
[10] H. Murakawa, Y. Onose, K. Ohgushi, S. Ishiwata, and Y. Tokura, J. Phys. Soc. Jpn. **77**, 043709 (2008).
[11] S. Seki, H. Murakawa, Y. Onose, and Y. Tokura, Phys. Rev. Lett. **103**, 237601 (2009).
[12] T. Kimura, J. C. Lashley, and A. P. Ramirez, Phys. Rev. B **73**, 220401(R) (2006).
[13] S. Kanetsuki, S. Mitsuda, T. Nakajima, D. Anazawa, H. A. Katori, and K. Prokes, J. Phys.: Condens. Matter **19**, 145244 (2007).
[14] S. Seki, Y. Yamasaki, Y. Shiomi, S. Iguchi, Y. Onose, and Y. Tokura, Phys. Rev. B **75**, 100403(R) (2007).
[15] N. Terada, T. Nakajima, S. Mitsuda, H. Kitazawa, K. Kaneko, and N. Metoki, Phys. Rev. B **78**, 014101 (2008).
[16] T. Nakajima, S. Mitsuda, S. Kanetsuki, K. Prokes, A. Podlesnyak, H. Kimura, and Y. Noda, J. Phys. Soc. Jpn. **76**, 043709 (2007).
[17] T. Nakajima, S. Mitsuda, K. Takahashi, M. Yamano, K. Masuda, H. Yamazaki, K. Prokes, K. Kiefer, S. Gerischer, N. Terada, H. Kitazawa, M. Matsuda, K. Kakurai, H. Kimura, Y. Noda, M. Soda, M. Matsuura, and K. Hirota, Phys. Rev. B **79**, 214423 (2009).
[18] T. Nakajima, S. Mitsuda, S. Kanetsuki, K. Tanaka, K. Fujii, N. Terada, M. Soda, M. Matsuura, and K. Hirota, Phys. Rev. B **77**, 052401 (2008).
[19] T. R. Zhao, M. Hasegawa, and H. Takei, J. Cryst. Growth **166**, 408 (1996).
[20] H. Mitamura, S. Mitsuda, S. Kanetsuki, H. A. Katori, T. Sakak-

ibara, and K. Kindo, J. Phys. Soc. Jpn. **76**, 094709 (2007).
[21] N. Terada, S. Mitsuda, H. Ohsumi, and K. Tajima, J. Phys. Soc. Jpn. **75**, 023602 (2006).
[22] F. Ye, Y. Ren, Q. Huang, J. A. Fernandez-Baca, P. Dai, J. W. Lynn, and T. Kimura, Phys. Rev. B **73**, 220404(R) (2006).
[23] N. Terada, Y. Tanaka, Y. Tabata, K. Katsumata, A. Kikkawa, and S. Mitsuda, J. Phys. Soc. Jpn. **75**, 113702 (2006).
[24] T. Nakajima, S. Mitsuda, T. Inami, N. Terada, H. Ohsumi, K. Prokes, and A. Podlesnyak, Phys. Rev. B **78**, 024106 (2008).
[25] Although the magnetic field was not exactly parallel to the c axis as mentioned in Sec. II, we consider that the in-plane component of the magnetic field hardly affected the magnetic ordering in this system, because the direction of the in-plane component of the magnetic field is parallel to the q' vector of the $(q,q,\frac{3}{2})$ domain.
[26] N. Terada, S. Mitsuda, T. Fujii, K. Soejima, I. Doi, H. A. Katori, and Y. Noda, J. Phys. Soc. Jpn. **74**, 2604 (2005).
[27] N. Terada, T. Kawasaki, S. Mitsuda, H. Kimura, and Y. Noda, J. Phys. Soc. Jpn. **74**, 1561 (2005).
[28] Note that the two reflections in the FE-ICM phase should be properly assigned as $(0,q,\frac{1}{2})$ and $(0,1-q,\frac{1}{2})$ using the monoclinic basis employed in the previous works. However, in this paper, we employed the conventional hexagonal basis in order to describe the directions of the magnetic modulation wave vectors of the three q domains.
[29] N. Terada, Y. Narumi, Y. Sawai, K. Katsumata, U. Staub, Y. Tanaka, A. Kikkawa, T. Fukui, K. Kindo, T. Yamamoto, R. Kanmuri, M. Hagiwara, H. Toyokawa, T. Ishikawa, and H. Kitamura, Phys. Rev. B **75**, 224411 (2007).
[30] N. Terada, S. Mitsuda, K. Prokes, O. Suzuki, H. Kitazawa, and H. A. Katori, Phys. Rev. B **70**, 174412 (2004).
[31] T. T. A. Lummen, C. Strohm, H. Rakoto, A. A. Nugroho, and P. H. M. van Loosdrecht, Phys. Rev. B **80**, 012406 (2009).
[32] G. Quirion, M. L. Plumer, O. A. Petrenko, G. Balakrishnan, and C. Proust, Phys. Rev. B **80**, 064420 (2009).
[33] K. Momma and F. Izumi, J. Appl. Crystallogr. **41**, 653 (2008).